AD-A149 760 HETEROCONTACT EFFECTS IN POINT CONTACT ELECTRON-PHONON SPECTROSCOPY OF TH..(U) CORNELL UNIV ITHACA NY LAB OF ATOMIC AND SOLID STATE PHYSICS.. H U BARANGER ET AL. 1/1

UNCLASSIFIED 15 DEC 84 TR-6 N00014-82-K-0576 F/G 7/2 NL

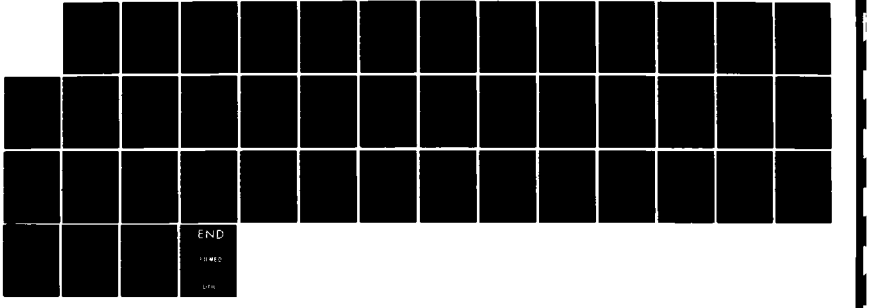

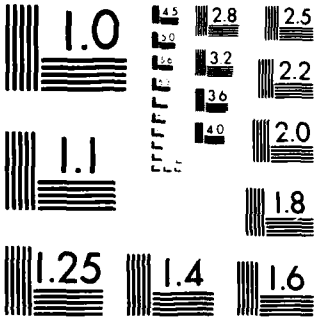

MICROCOPY RESOLUTION TEST CHART
NATIONAL BUREAU OF STANDARDS 1963 A

OFFICE OF NAVAL RESEARCH

Research Contract No. N00014-K-0576

TECHNICAL REPORT No. 6

HETEROCONTACT EFFECTS IN POINT CONTACT ELECTRON-PHONON SPECTROSCOPY OF THE ALKALI METALS

by

H. U. Baranger, A. H. MacDonald and C. R. Leavens

Prepared for Publication

in

Physical Review B

Laboratory of Atomic and Solid State Physics
Cornell University
Ithaca, NY 14853

SECURITY CLASSIFICATION OF THIS PAGE (When Data Entered)

REPORT DOCUMENTATION PAGE		READ INSTRUCTIONS BEFORE COMPLETING FORM
1. REPORT NUMBER: 6	2. GOVT ACCESSION NO.	3. RECIPIENT'S CATALOG NUMBER
4. TITLE (and Subtitle): Heterocontact effects in point contact electron-phonon spectroscopy of the alkali metals.		5. TYPE OF REPORT & PERIOD COVERED: Interim 6. PERFORMING ORG. REPORT NUMBER
7. AUTHOR(s): H. U. Baranger, A. H. MacDonald and C. R. Leavens		8. CONTRACT OR GRANT NUMBER(s): N00014-82-K-0576
9. PERFORMING ORGANIZATION NAME AND ADDRESS: Laboratory of Atomic and Solid State Physics, Cornell University, Ithaca, N.Y. 14853		10. PROGRAM ELEMENT, PROJECT, TASK AREA & WORK UNIT NUMBERS
11. CONTROLLING OFFICE NAME AND ADDRESS: Office of Naval Research, Washington, D. C. 10360		12. REPORT DATE: December 15, 1985 13. NUMBER OF PAGES: 40
14. MONITORING AGENCY NAME & ADDRESS(if different from Controlling Office)		15. SECURITY CLASS. (of this report): Unclassified 15a. DECLASSIFICATION/DOWNGRADING SCHEDULE

16. DISTRIBUTION STATEMENT (of this Report)

Approved for public release; distribution unlimited.

17. DISTRIBUTION STATEMENT (of the abstract entered in Block 20, if different from Report)

18. SUPPLEMENTARY NOTES

Submitted to Physical Review B.

19. KEY WORDS (Continue on reverse side if necessary and identify by block number)

20. ABSTRACT (Continue on reverse side if necessary and identify by block number)

For a small contact between two different materials (a hetero-contact), we derive the free electron expression for the electron-phonon spectral function determined from the measured I-V characteristic. The heterocontact spectral function differs strikingly from the homocontact spectral function in that it excludes scattering through angles less than a minimum angle in the larger bandwidth material. We calculate realistic heterocontact spectra for pairs of alkali metals. If in a given pair of alkalis the smaller bandwidth material is

DD FORM 1473 EDITION OF 1 NOV 65 IS OBSOLETE

S/N 0102-014-6601

SECURITY CLASSIFICATION OF THIS PAGE (When Data Entered)

(20 continued)

replaced by one with a still smaller bandwidth, the size of the signal from the larger bandwidth material decreases (sometimes dramatically), and the part of the spectrum due to scattering by $2k_F$ phonons is relatively enhanced.

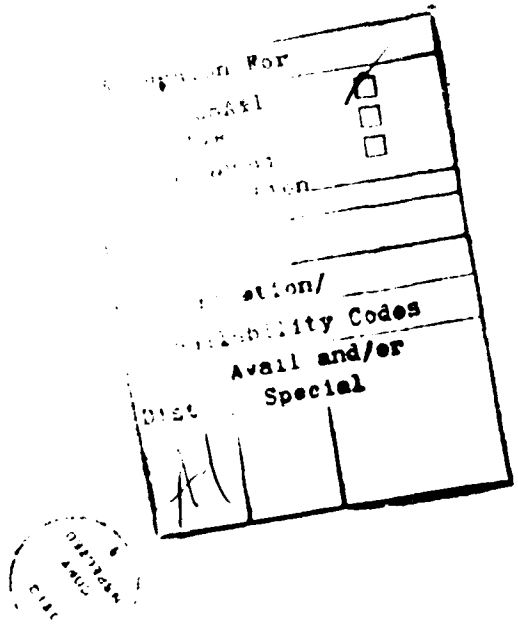

(3)

Heterocontact effects in point contact electron-phonon spectroscopy of the alkali metals

H. U. Baranger

Laboratory of Atomic and Solid State Physics, Cornell University, Ithaca, N. Y. 14853

A. H. MacDonald and C. R. Leavens

Division of Microstructural Science, National Research Council of Canada, Ottawa, Canada K1A OR6

ABSTRACT

For a small contact between two different materials (a heterocontact), we derive the free electron expression for the electron-phonon spectral function determined from the measured I-V characteristic. The heterocontact spectral function differs strikingly from the homocontact spectral function in that it excludes scattering through angles less than a minimum angle in the larger bandwidth material. We calculate realistic heterocontact spectra for pairs of alkali metals. If in a given pair of alkalis the smaller bandwidth material is replaced by one with a still smaller bandwidth, the size of the signal from the larger bandwidth material decreases (sometimes dramatically), and the part of the spectrum due to scattering by $2k_F$ phonons is relatively enhanced.

PACS Numbers: 73.40.Jn, 72.15.Eb

I. Introduction

Point contact spectroscopy has been successfully used to study the electron-phonon interaction in a wide variety of metals,[1] including the alkali metals.[2,3] In this technique, one measures the derivatives of the I-V curve of a small contact between two bulk materials. If the size of the contact is smaller than the inelastic mean free path, the non-ohmic part of the resistance is proportional to a weighted average over the Fermi surface of the scattering rate at the applied voltage.[1,4] Most work to date has used contacts between the same material (homocontacts), and for this case the weight factor is well known (see Eq.(7) below).[4,5]

Contacts between two different materials (heterocontacts) differ from homocontacts in two important ways: the difference in Fermi velocity leads to reflection and refraction of electrons at the interface (kinematic effects), and the charge density at the interface scatters the electrons. Experiments done on heterocontacts[1,6,7] show phonon structure from both materials and are roughly consistent with adding the individual spectra of the two materials, but have not been subjected to a detailed shape analysis. Heterocontacts have been investigated theoretically using the methods developed for homocontacts. The distribution of electrons in a heterocontact in the approximation of no scattering has been calculated,[8] and interface scattering effects (modelled by a δ-function barrier) and kinematic effects for two materials with very different Fermi energies have been investigated.[9] However, the weight factor for electron-phonon scattering in the heterocontact case has not previously been calculated.

In this paper we find the weight factor for a heterocontact, taking into account the kinematic effects of the interface but not the interface scattering, and

calculate realistic point contact spectra for pairs of alkali metals. In deriving our expression for the weight factor we assume that both materials are free electron metals at zero temperature. (The experiments are usually done at low temperature.) We use the method of Kulik, Omel'yanchuk, and Shekter[4] in which one solves the Boltzmann equation to first order in the electron-phonon interaction. We find, first, that the weight factor for a heterocontact differs from that for a homocontact only in the larger bandwidth material. Second, in the larger bandwidth material, scattering through angles less than a minimum angle is excluded and the phase space for allowed scattering is reduced. Third, the overall magnitude of the spectrum from the larger bandwidth material decreases, sometimes dramatically, because of the smaller bandwidth material. Fourth, the portions of the spectrum with a high contribution from scattering by $2k_F$ phonons are enhanced relative to other portions of the spectrum.

In section II, we discuss the geometry of the contact and the current through the contact in the absence of scattering. Then we add the electron-phonon scattering and derive the weight factor in sections III and IV. Sections V and VI present the method of calculating the spectra of the alkali metals and the results, respectively. Finally, we summarize and comment on the possibility of more general applicability of our results (section VII).

II. Geometry and No Scattering Current

Throughout this paper, the geometry that we consider is an idealized form of the point contact geometry.[1] As shown in Figure 1(a), we consider two free-electron metals of differing densities, and hence bandwidth, joined at an interface

in the z=0 plane. The difference in bandwidth, $\Delta = \mu_1 - \mu_2$, is the intrinsic potential step seen by electrons crossing between material 1 and material 2. The interface is insulating except for a small round hole of radius a which represents the point contact.

Before discussing the distribution of electrons under an applied bias, we point out some important features of the equilibrium case. In equilibrium the distribution, $f(\vec{r},\vec{k})$, depends on $\vec{k}$ only through the kinetic energy, ϵ_k, and is given by the Fermi function appropriate to the material at the point $\vec{r}$:

$$f(\vec{r},\vec{k}) = \begin{cases} f_1^0(\epsilon) = \dfrac{1}{e^{\beta(\epsilon_k - \mu_1)}+1}, & \text{for } z<0 \\ f_2^0(\epsilon) = \dfrac{1}{e^{\beta(\epsilon_k - \mu_2)}+1}, & \text{for } z>0 \end{cases} \tag{1}$$

The crucial difference between a heterocontact and a homocontact is the intrinsic potential step between materials 1 and 2. This step affects electrons crossing between materials 1 and 2 in two important ways: an electron's momentum perpendicular to the step must be greater than a critical value in order to pass from material 1 to 2, and any electron crossing from material 2 to 1 gains perpendicular momentum at the step. We define a critical wavevector,

$$k_c = \sqrt{2m(\mu_1 - \mu_2)}/\hbar = \sqrt{2m\Delta}/\hbar, \tag{2}$$

in terms of which all the kinematic effects of the heterocontact can be written: an electron in material 1 must have $k_z > k_c$ in order to enter material 2, and an electron which has crossed from material 2 to 1 must have $k_z < -k_c$. Figure 1(b) shows the equilibrium distribtuion and indicates which electrons will cross or have crossed the potential step.

Turning now to the situation when a voltage is applied, we first consider the limit when there is no scattering and obtain the distribution, $f^{ns}(\vec{r},\vec{k})$, both by a qualitative argument[8] and from the Boltzmann equation. We restrict ourselves to the case of a small applied voltage, $|eV| \ll \mu_2$, applied so that the net electron flow is from material 1 to 2 (i.e. $V>0$). Our final results are equally valid if the net electron flow is from material 2 to 1. In this case the trajectories of the electrons are essentially straight within either material because the applied potential drop, which is concentrated near the hole because of the constriction resistance, is not large enough to bend electrons near the Fermi level, the only electrons that contribute to the net current. An electron crossing the hole in the z=0 plane is, of course, bent: its parallel wave vector is conserved, but k_z changes in order to accomadate the change in energy, $\pm\Delta$.

Because electrons crossing the hole from left to right gain kinetic energy from the applied field while ones crossing from right to left lose kinetic energy, at any point in space electrons originally from the Fermi level of material 1 will have eV more energy than electrons originally from the Fermi level of material 2. Thus the distribution of electrons at a point $\vec{r}$ is broken into two distinct regions in $\vec{k}$ with different filling levels: the maximum energy of electrons from material 1 is eV greater than the maximum energy of electrons from material 2.

The geometry of the contact determines the size of each of these regions in $\vec{k}$. Given a point $\vec{r}$ in material 1, the number of electrons from material 2 and their $\hat{k}$ are restricted by the solid angle subtended by the hole from $\vec{r}$; we let $\Omega(\vec{r})$ be the set of $\hat{k}$ that point at the hole from $\vec{r}$. However, because of the internal potential step, all electrons with $|k_z| < k_c$ in material 1 originated in

material 1 (see Eq. (2)). Thus in material 1, the solid angle restricts the electrons from material 2 only if this restriction is more severe than simply $k_z < -k_c$. On the other hand, given a point in material 2, the only restriction on the electrons from material 1 is the solid angle subtended by the hole, as in the case of a homocontact. Figure 2 shows the distribution without scattering, $f^{ns}(\vec{r},\vec{k})$, obtained by applying the solid angle restriction while keeping in mind that $k_z < -k_c$ for any electron in material 1 which came from material 2.

To obtain this same result formally, we follow the method of Kulik, et al.[4] and solve the collisionless Boltzmann equation where the force acting on an electron, $\vec{F}(\vec{r})$, has a contribution both from the applied potential energy, $U(\vec{r})$ (defined so U=0 at the hole), and from the internal step Δ:

$$\frac{\vec{F}(\vec{r})}{\hbar}\cdot\frac{\partial f^{ns}}{\partial \vec{k}} + \frac{\hbar\vec{k}}{m}\cdot\frac{\partial f^{ns}}{\partial \vec{r}} = 0 \qquad (3)$$

$$\vec{F}(\vec{r}) = -\frac{\partial}{\partial \vec{r}}\left(U(\vec{r}) + \Delta\theta(z)\right).$$

Integration along a trajectory Γ defined by $\dot{\vec{r}} = \hbar\vec{k}/m$ and $\dot{\vec{k}} = \vec{F}(\vec{r})/\hbar$ transforms the Boltzmann equation to the set of equations $df^{ns}(\vec{r}(t),\vec{k}(t))/dt = 0$, there being one equation for each trajectory Γ. The solution of these equations is clearly that f^{ns} is constant along each trajectory.

The value of f^{ns} along any given trajectory depends on which side of the contact the particle originated and on the boundary condition, which we take to be $f^{ns} \to f_1^0$ as $z \to -\infty$ and $f^{ns} \to f_2^0$ as $z \to +\infty$. States which originate in material 1 are filled to a higher energy than those which originate in material 2 because the Fermi level as $z \to -\infty$ is eV above the Fermi level as $z \to +\infty$. We denote by $E_{>,i}(\vec{r})$ the maximum kinetic energy of electrons in material i at

point $\vec{r}$ which came from material 1 and call this energy the higher filling level. Likewise, we denote by $E_{<,i}(\vec{r})$ the maximum kinetic energy of electrons in material i at point $\vec{r}$ which came from material 2 and call this energy the lower filling level. The filling levels vary in space because of the applied potential and the expressions $E_{<,i}(\vec{r})=\mu_i-U(\vec{r})-eV/2$ and $E_{>,i}(\vec{r})=\mu_i-U(\vec{r})+eV/2$ relate the lower and higher filling levels respectively to the applied potential and the Fermi energies. In terms of these filling levels the following two statements completely specify f^{ne}. (1) If the state $\vec{k}$ at point $\vec{r}$ came from material 1, it is filled (that is $f^{ne}(\vec{r},\vec{k})=1$) if $\epsilon_k<E_{>,i}(\vec{r})$ and empty otherwise ($f^{ne}(\vec{r},\vec{k})=0$). (2) If the state $\vec{k}$ at point $\vec{r}$ came from material 2, it is filled if $\epsilon_k<E_{<,i}(\vec{r})$ and empty otherwise.

An explicit expression for $f^{ne}(\vec{r},\vec{k})$ requires a self-consistent solution for $U(\vec{r})$, the paths Γ and the density $n(\vec{r})=\int f(\vec{r},\vec{k})\,d^3k/4\pi^3$, which is coupled back to $U(\vec{r})$ through Poisson's equation. We side-step the question of self-consistency by assuming, as above, that the paths of the particles are straight lines within each material and bend at the interface. This assumption leads to an explicit form for $f^{ne}(\vec{r},\vec{k})$:

$$f^{ne}(\vec{r},\vec{k})=\begin{cases} f_1^0(\epsilon_k+U(\vec{r})-eV/2),\ z<0,\ -\hat{k} \text{ not in } \Omega(\vec{r}) \text{ or } k_z>-k_z \\ f_1^0(\epsilon_k+U(\vec{r})+eV/2),\ z<0,\ -\hat{k} \text{ in } \Omega(\vec{r}) \text{ and } k_z<-k_z \\ f_2^0(\epsilon_k+U(\vec{r})-eV/2),\ z>0,\ -\hat{k} \text{ in } \Omega(\vec{r}) \\ f_2^0(\epsilon_k+U(\vec{r})+eV/2),\ z>0,\ -\hat{k} \text{ not in } \Omega(\vec{r}) \end{cases}, \qquad (4)$$

where $\Omega(\vec{r})$ is the set of $\hat{k}$ that point at the hole from $\vec{r}$.

The feature of $f^{ne}(\vec{r},\vec{k})$ for a heterocontact (Eq. (4)) which distinguishes it from the homocontact case is the additional restriction in material 1: only states

with $k_z < -k_c$ are filled to the lower filling level $E_{<,1}$ because all electrons from material 2 must have $k_z < -k_c$. The distribution in material 2 is independent of material 1 and so is identical to the distribution in a homocontact made from material 2 at the same applied voltage.[8] Consequently, all the effects of the bi-material nature of the contact are felt in material 1 and are determined by the critical wavevector k_c.

The current implied by the distribution in Eq. (4) can be calculated from $\vec{J} = -e \int \vec{v} f(\vec{r}, \vec{k}) d^3k / 4\pi^3$ and is the same as in a homocontact made from material 2:[8]

$$J = \left(\frac{e^2 a^2 k_{F2}^2}{4\pi\hbar} \right) V . \tag{5}$$

III. Electron Phonon-Scattering: Discussion of the main effects

The general effect of electron-phonon scattering is to modulate the current through the contact because the electron scattering is inelastic. In order for scattering in a given channel, $\vec{k} \rightarrow \vec{k}'$, to affect the current, two conditions must be satisfied: there must be available initial states ($\vec{k}$) and final states ($\vec{k}'$), and the electron must either scatter out of or into a state that contributes to the current through the hole. These two conditions lead to restrictions both on the energies of the final and initial states, and on $\hat{k}$ and $\hat{k}'$ because of the geometry of the point contact (which in our case is a simple circular hole). The restrictions on $\hat{k}$ and $\hat{k}'$ mean that each scattering channel contributes to the change in current, ΔI, with a different weight. In the rest of this section, we deduce the restrictions on energies and on $\hat{k}$ and $\hat{k}'$ first for material 2 and then for

material 1, and we present the weight factor, $W(\vec{k},\vec{k}')$, and the change in current that these restrictions imply. Section IV contains a more detailed derivation of the weight factor. Because we assume that the mean free path is much larger than the size of the hole, electron-phonon scattering does not greatly perturb the distribution of electrons. Thus, the restrictions on $\vec{k}$ and $\vec{k}'$ can be deduced by looking at $f^{neq}(\vec{r},\vec{k})$ in each material (see Fig. 2). At zero temperature, only phonon emmission occurs and hence the energy of the initial state must be greater than that of the final state.

In material 2, the energy of an initial state must be less than the higher filling level, $E_{<,2}(\vec{r})$, and the energy of a final state must be greater than the lower filling level $E_{>,2}(\vec{r})$. Thus the maximum energy difference between initial and final states, and hence the maximum phonon energy, is the applied voltage $eV = E_{<,2}(\vec{r}) - E_{>,2}(\vec{r})$. In order to have the initial energy greater than the final energy (phonon emission), the initial electron $\vec{k}$ must have come through the hole from material 1 ($-\vec{k}$ in $\Omega(\vec{r})$). And in order to affect the current, the electron must go back through the hole, which restricts the final states to $\vec{k}'$ in $\Omega(\vec{r})$. Thus in material 2 at a point $\vec{r}$, the current is affected by scattering from states near the Fermi level with $-\vec{k}$ in $\Omega(\vec{r})$ to states with $\vec{k}'$ in $\Omega(\vec{r})$ where $\epsilon_k - \epsilon_{k'} \leq eV$. The situation described here for material 2 is identical to the case of a homocontact of material 2,[4,8] and hence the current modulation caused by the scattering in material 2 is identical to that in a homocontact.

In material 1, the energy of an initial state must be less than the higher filling level, $E_{<,1}(\vec{r})$, and the energy of a final state must be greater than the lower filling level $E_{>,1}(\vec{r})$. Thus as in material 2, the maximum phonon energy

is the applied voltage $eV = E_{>,1}(\vec{r}) - E_{<,1}(\vec{r})$. In order to have the initial energy greater than the final energy, the final state $\vec{k}'$ must come from material 2, which implies that $k_z' < -k_c$ because of the internal potential step as well as that $-\hat{k}'$ in $\Omega(\vec{r})$. And in order to affect the current, the initial electron must be one which would go through the hole if it did not scatter, which implies $k_z > k_c$ and $\hat{k}$ in $\Omega(\vec{r})$. Thus in material 1 the scattering that affects the current is that from states near the Fermi level with $\hat{k}$ in $\Omega(\vec{r})$ and $k_z > k_c$ to states with $-\hat{k}'$ in $\Omega(\vec{r})$ and $k_z' < -k_c$ where $\epsilon_k - \epsilon_{k'} \leq eV$.

The difference between the restrictions in material 1 and those in the case of a homocontact is the two additional restrictions $k_z > k_c$ and $k_z' < -k_c$. Notice the crucial role played by the critical wavevector k_c (defined in Eq. (2)). These additional restrictions imply two important effects. First, scattering channels in which the perpendicular momentum changes by less than $2k_c$ do not change the current through the hole. Thus, the only detectable scattering events are those whose scattering angle $\Theta_{\vec{k},\vec{k}'} = \cos^{-1}(\hat{k} \cdot \hat{k}')$ is greater than a minimum scattering angle Θ_{min} defined by $\sin(\Theta_{min}/2) = k_c / k_{F1}$ (see Fig. 2). Θ_{min} eliminates small angle scattering from the measured signal and enhances the relative importance of large angle scattering. Second, for scattering angles larger than Θ_{min}, the restrictions on k_z and k_z' reduce the total amount of scattering contributing to the change in current compared to the homocontact case. Thus the magnitude of ΔI in the heterocontact will be smaller than in the corresponding homocontact.

We summarize these arguments by giving an expression for the change in current which is derived in more detail below. The change in current because of scattering in material i is usually written in terms of a spectral function $G^{(i)}(\omega)$,

which in turn is written in terms of the phonon frequencies $\omega_q^{(i)}$, the matrix element $g_{kk'}^{(i)}$ (which we assume depends only on $\vec{q}=\vec{k}-\vec{k}'$), and the density of states at the Fermi level $N_0^{(i)}=mk_{Fi}/\hbar^2\pi^2$:

$$\Delta I^{(i)} = e\left(\frac{2\pi}{\hbar}\right)2N_0^{(i)}\left(\frac{a^3}{3}\right)\int_{E_{<,i}(0)}^{E_{<,i}(0)-eV} d\epsilon \int_{E_{<,i}(0)}^{\epsilon} d\epsilon' \, G^{(i)}(\epsilon-\epsilon') \tag{6a}$$

$$G^{(i)}(\omega) = \frac{1}{4\pi^3 N_0^{(i)}}\left(\frac{1}{2\pi}\right)^3 \int \frac{dS_k}{\hbar\,|\,v_k\,|}\int \frac{dS_{k'}}{\hbar\,|\,v_{k'}\,|} \tag{6b}$$

$$\times\,|\,g_{k,k'}^{(i)}\,|^2\delta(\omega-\hbar\omega_{k-k'}^{(i)})\,W^{(i)}(\hat{k},\hat{k}')\,.$$

Here $W^{(i)}(\hat{k},\hat{k}')$ is the weight factor due to geometrical effects and the integrals over dS_k and $dS_{k'}$ are over the Fermi surface. For the contribution to ΔI from scattering in material 2,

$$W^{(2)}(\hat{k},\hat{k}') = \theta(-k_z)\theta(k_z')\times\left\{8\frac{|\,k_z\,|\cdot|\,k_z'\,|}{|\,k_z'\vec{k}-k_z\vec{k}'\,|}\right\}, \tag{7}$$

which is one-half of the homocontact weight factor[4] because the right side of a homocontact contributes one-half of the signal. In material 1, the weight factor is

$$W^{(1)}(\hat{k},\hat{k}') = \theta(k_z-k_c)\theta(-k_c-k_z')\times\left\{8\frac{|\,k_z\,|\cdot|\,k_z'\,|}{|\,k_z'\vec{k}-k_z\vec{k}'\,|}\right\}. \tag{8}$$

For comparison, the Eliashberg spectral function of superconductivity theory uses $W(\hat{k},\hat{k}')=1$.

The energy integrals in Eq.(6a) mean that as the applied voltage V increases, more phonon channels contribute so that the resistance of the contact increases.

In the weight factors (Eq. (7) and (8)), the θ- functions take care of the restrictions on k_z and k_z' which is where the homocontact and heterocontact weight factors differ, and the solid angle restriction results in the expression in braces in both equations (derived in the next section). We note that the spectral function $G^{(i)}(\omega)$ does not depend on the sign of the voltage; forward and reverse bias measure the same spectral function.

IV. Electron-Phonon Scattering: derivation of the weight factor

In this section we give a detailed derivation of Eqs. (6)-(8). We follow the method of Kulik, et al.[4] which consists of solving the Boltzmann equation using $f^{ne}(\vec{r},\vec{k})$ in the collision integral:

$$\frac{\vec{F}(\vec{r})}{\hbar}\cdot\frac{\partial f}{\partial \vec{k}} + \frac{\hbar\vec{k}}{m}\cdot\frac{\partial f}{\partial \vec{r}} = I^{(i)}[f^{ne}(\vec{r},\vec{k})],\ i=1,2\,. \tag{9}$$

The scattering integral $I^{(i)}$ is that appropriate to the material at the point $\vec{r}$. This equation can be solved by writing $f = f^{ne} + \delta f$ and integrating the resulting equation along the path Γ defined above which yields[4,10]

$$\delta f\,(\vec{r}(t),\vec{k}(t)) = \int_{-\infty}^{t} dt'\, I^{(i)}[f^{ne}(\vec{r}(t'),\vec{k}(t')]. \tag{10}$$

The change in current, obtained by multiplying by v_{kz} and integrating over both $\vec{k}$ and the hole, is

$$\Delta I = -e\int_{hole} d^2r \sum_{k} v_{kz}^{(i)} \int_{-\infty,\Gamma}^{t} dt'\, I^{(i)}[f^{ne}(\vec{r}(t'),\vec{k}(t'))],\ i=1,2 \tag{11}$$

where t is the time at which the particle reaches the hole. Note that $v_{kz}^{(i)}$ is

material dependent and that ΔI can be evaluated either on the left side of the hole (in material 1) or on the right side (in material 2). For convenience, we choose to evaluate ΔI so that for any $\vec{k}$, Γ is entirely in material 1 or material 2. Thus, for electrons from the right ($v_{kz}<0$), we evaluate ΔI in material 2. For electrons from the left ($v_{kz}>0$), we evaluate ΔI in material 1 with the condition that only electrons which would be able to get into material 2 are considered, $v_{kz}>\hbar k_c/m$. Our expression for the current, therefore, is

$$\Delta I = \Delta I^{(1)}+\Delta I^{(2)}$$

$$= -e\int_{hole} d^2r \sum_k \theta(k_z-k_c)\, v_{kz}^{(1)} \int_{-\infty,\Gamma}^{t} dt'\, I^{(1)}[f^{ne}(\vec{r}(t'),\vec{k}(t'))] \qquad (12)$$

$$-e\int_{hole} d^2r \sum_k \theta(-k_z)\, v_{kz}^{(2)} \int_{-\infty,\Gamma}^{t} dt'\, I^{(2)}[f^{ne}(\vec{r}(t'),\vec{k}(t'))] .$$

To simplify equation (12) we combine the integral over the hole and over time into a single volume integral over the half tube, $T(\vec{k})$, parallel to $\vec{k}$ which intersects the hole and which lies upstream from the hole (see Fig. 3). The electrons which can scatter are close to the Fermi level and have straight paths, so that $dt' = ds/|\vec{v}_k(s)| = ds/v_F$ where s is the distance along the path. The Jacobean for converting from $d^2r\,ds$ to d^3r is $|v_{kz}/v_F|$, so that the current is:[11]

$$\Delta I = -e\sum_k \int_{T(\vec{k})} d^3r \left\{ \theta(k_z-k_c) I^{(1)}[f^{ne}(\vec{r},\vec{k})] - \theta(-k_z) I^{(2)}[f^{ne}(\vec{r},\vec{k})] \right\}. \qquad (13)$$

The electron-phonon scattering integral,

$$I^{(i)}[f^{ne}(\vec{r},\vec{k})] = \frac{2\pi}{\hbar}\sum_{k'} |g_{k,k'}^{(i)}|^2 \times$$

$$\left\{ f^{ne}(\vec{r},\vec{k}')[1-f^{ne}(\vec{r},\vec{k})]\delta(\epsilon_k - \epsilon_{k'} + \hbar\omega_{k-k'}) \right. \tag{14}$$

$$\left. - f^{ne}(\vec{r},\vec{k})[1-f^{ne}(\vec{r},\vec{k}')]\delta(\epsilon_k - \epsilon_{k'} - \hbar\omega_{k-k'}) \right\},$$

in which we assume that $g_{k,k'}$ depends only on $\vec{q}=\vec{k}-\vec{k}'$, places constraints on the possible energies through the Fermi factors. In the first term (into the beam), $\epsilon_{k'} > \epsilon_k$ because only phonon emission is included (T=0), $\epsilon_{k'} < eV + E_{<,i}(\vec{r})$ in order to have an initial state, and $\epsilon_k > E_{<,i}(\vec{r})$ in order to have an empty final state. Similarly for the second term of the scattering integral, $E_{<,i}(\vec{r}) < \epsilon_{k'} < \epsilon_k < eV + E_{<,i}(\vec{r})$.

The Fermi factors of the scattering integral also contain geometrical restrictions on $\hat{k}$ and $\hat{k}'$. In material 1, because of the restriction $k_z > k_c$ in Eq.(13), $\vec{k}$ is necessarily a filled state, so that only the second term in the scattering integral contributes (out of the beam). Looking at the distribution $f^{ne}(\vec{r},\vec{k}')$ (Figure 2), all possible empty final states have $k_z' < -k_c$, and have $-\hat{k}'$ in $\Omega(\vec{r})$. Similarly in material 2, the restriction in Eq. (13) implies that $\vec{k}$ is an empty final state, and hence only the first term of the scattering integral contributes (into the beam). All initial states have $k_z' > 0$ and have $-\hat{k}'$ in $\Omega(\vec{r})$. The restrictions on k_z can be included by using θ functions. The restriction $-\hat{k}'$ in $\Omega(\vec{r})$ can be included in the region of spatial integration because at any point $\vec{r}$, the state $\vec{k}'$ is available as a final (initial) state in material 1 (2) only if $\vec{r}$ is in the half tube,

$\overline{T}(\vec{k}')$, parallel to $\vec{k}'$ which intersects the hole and is downstream from the hole (the complement of $T(\vec{k})$, see Fig. 3). Thus, restricting the region of spatial integration to the intersection of $T(\vec{k})$ and $\overline{T}(\vec{k}')$ satisfies $-\hat{k}$ in $\Omega(\vec{r})$.

With the energy and geometric restrictions included, the expressions for the change in current caused by scattering in material 1 and material 2 are:

$$\Delta I^{(1)} = +e\frac{2\pi}{\hbar}\int_{E_{<,1}(0)}^{E_{<,1}(0)+eV}\frac{d\epsilon}{4\pi^3}\int_{E_{<,1}(0)}^{\epsilon}\frac{d\epsilon'}{4\pi^3}\int\frac{dS_k}{\hbar\mid v_k\mid}\int\frac{dS_{k'}}{\hbar\mid v_{k'}\mid}\mid g_{k,k'}^{(1)}\mid^2$$

$$\times\delta(\epsilon_k-\epsilon_{k'}-\hbar\omega_{k-k'}^{(1)})\left\{\theta(k_z-k_c)\theta(-k_c-k_z')\int_{T(\vec{k})\bigcap\overline{T}(\vec{k}')}d^3r\right\} \qquad (15a)$$

$$\Delta I^{(2)} = +e\frac{2\pi}{\hbar}\int_{E_{<,2}(0)}^{E_{<,2}(0)+eV}\frac{d\epsilon'}{4\pi^3}\int_{E_{<,2}(0)}^{\epsilon'}\frac{d\epsilon}{4\pi^3}\int\frac{dS_k}{\hbar\mid v_k\mid}\int\frac{dS_{k'}}{\hbar\mid v_{k'}\mid}\mid g_{k,k'}^{(2)}\mid^2$$

$$\times\delta(\epsilon_k-\epsilon_{k'}+\hbar\omega_{k-k'}^{(2)})\left\{\theta(-k_z)\theta(k_z')\int_{T(\vec{k})\bigcap\overline{T}(\vec{k}')}d^3r\right\} \qquad (15b)$$

The spatial dependence of $E_{i,<}(\vec{r})$ has been neglected because we assume that the electron-phonon interaction depends only on $\vec{q}=\vec{k}-\vec{k}'$ and not on ϵ_k or $\epsilon_{k'}$ independently.

The volume of the intersecting tubes $T(\vec{k})$ and $\overline{T}(\vec{k})$ which is necessary to evaluate Eq. (15) has been calculated by Kulik, et al.[1]:

$$\int_{T(\vec{k})\bigcap\overline{T}(\vec{k}')}d^3r = \frac{8a^3}{3}\cdot\frac{\mid k_z\mid\cdot\mid k_z'\mid}{\mid k_z'\vec{k}-k_z\vec{k}'\mid}. \qquad (16)$$

Taking the second derivative of the current enhances the sensitivity to the phonons and yields :

$$\frac{d^2I}{dV^2} = \frac{4}{3\pi}\cdot\frac{e^3m^2a^3}{\hbar^4}\cdot\left[v_{F1}G^{(1)}(eV) - v_{F2}G^{(2)}(eV)\right] \qquad (17)$$

where $G^{(1)}$ and $G^{(2)}$ are given in Eqs. (6)-(8).

This completes the derivation of the weight factor in the heterocontact case (Eqs. (7) and (8)). The derivation can be repeated for the case of net electron flow from material 2 to material 1 and yields the same result for d^2I/dV^2 in the case $|eV| \ll \mu_2$. We now turn to the effect that this weight factor has on point contact spectra.

V. Method for Calculating Alkali Spectra

In order to investigate the effect of the heterocontact weight factor on realistic point contact spectra, we carried out detailed calculations of the spectra for point contacts made from pairs of the alkali metals Li, Na, K, Rb, and Cs. The alkali metals are particularly appropriate for illustrating the arguments given above because they have nearly spherical Fermi surfaces and effective masses close to the free electron value. The fact that the Li and Cs effective masses are larger than the free electron value[12] could influence our quntitative results;[13] however, we wish in this paper to emphasize the qualitative effects of the heterocontact weight factor and these should not be significantly affected by the effective mass in Li and Cs. In addition, the alkalis have a sufficiently complex phonon structure to illustrate nicely the main effects of the additional restrictions on scattering in material 1 : the reduced phase space available, and the minimum

scattering angle.

The heterocontact weight factor differs from that for a homocontact only for scattering in material 1, so we will normalize the total spectral function that we calculate, $G(\omega)$, using the velocity v_{F1} :

$$G(\omega) = G^{(1)}(\omega) + \frac{v_{F2}}{v_{F1}} G^{(2)}(\omega) \tag{18}$$

where $G^{(i)}(\omega)$ is defined in Eq. (6). The minimum scattering angle Θ_{min} (see Fig. 2) determines how different the heterocontact spectrum will be from the average of the two homocontact spectra. Table I lists the values of Θ_{min} used in this work for all combinations of the five alkalis studied: Θ_{min} ranges from 41.7^0 for a K, Rb contact to 109.2^0 for a Li, Cs contact.

To perform the calculations we use the same method as in reference 14 which we summarize here. We assume that the Fermi surface is spherical and express the electron-phonon matrix element in terms of the ionic mass and number density (M and N), the phonon energies and polarization vectors ($\omega_{\vec{q},\lambda}$, $\vec{e}_{\vec{q},\lambda}$), and the screened electron-ion pseudopotential form factor ($V(|\vec{q}|)$), by using the one-orthogonalized-plane-wave result :

$$|g_{\vec{k},\vec{k}',\lambda}|^2 = \frac{\hbar(\vec{k}-\vec{k}')\cdot\vec{e}_{\vec{k}-\vec{k}',\lambda}|^2 V^2(|\vec{k}-\vec{k}'|)}{2MN\omega_{\vec{k}-\vec{k}',\lambda}} . \tag{19}$$

A first principles calculation of the lattice dynamics and electron-phonon interaction[15] developed originally by Dagens, Rasolt and Taylor[16], provides the inputs $\omega_{\vec{q},\lambda}$, $\vec{e}_{\vec{q},\lambda}$, and $V(|\vec{q}|)$ to our calculation. The pseudopotential is a result of fitting the linear response of the charge density induced about an isolated ion embedded in an electron gas to Dagen's full nonlinear calculation of the same

quantity. This pseudopotential has proven successful in calculations of various properties of Na, K, and Rb,[17] giving us confidence in our results for these metals. While the one-OPW result is not strictly valid for Li or Cs, we believe that our qualitative results should apply to these metals as well.

In previous calculations of the homocontact spectral functions of the alkalis,[14] it has been shown that inspite of the large anisotropy of the phonons in these materials, the spectral function does not vary greatly as the crystal face on which the contact is made changes. Hence we neglect the anisotropy of the phonons by calculating the average of the spectral function over all crystal directions of the contact. This is equivalent to using a weight factor which depends only on the angle between $\hat{k}$ and $\hat{k}'$, $\Theta_{\hat{k},\hat{k}'}=\cos^{-1}(\hat{k}\cdot\hat{k}')$, or equivalently only on $q=2k_F\sin(\Theta_{\hat{k},\hat{k}'}/2)$. Such a weight factor is simply the average of $W(\hat{k},\hat{k}')$ given in Eqs. (7) and (8) over all $\hat{k}$ and $\hat{k}'$ keeping $\hat{k}\cdot\hat{k}'$ fixed. In material 2 this average weight factor is the same as that for the right side of a homocontact which is simply one-half of the full homocontact result:[5]

$$W^{(2)}(q)=\frac{1}{4}(1-\Theta_{\hat{k},\hat{k}'}/\tan\Theta_{\hat{k},\hat{k}'})\,. \tag{20}$$

In figure 4 we show the ratio of the average weight factor in material 1, $W^{(1)}(q)$, calculated numerically to $W^{(2)}(q)$ given in Eq. (20) for four values of the critical wavevector, k_c. Notice three important features of the heterocontact weight factor. (1) $W^{(1)}(q)$ is zero for $q<2k_c$ since scattering through an angle less than $\Theta_{\min}$ in material 1 does not affect the current through the hole. (2) $W^{(1)}(q)$ is less than $W^{(2)}(q)$ for all q because the phase space for phonon emission with $q>2k_c$ is smaller. (3)The (integrable) singularity in $W^{(2)}(q)$ at $q=2k_F$

remains in $W^{(1)}(q)$, but the strength of the singularity decreases because fewer $2k_F$ scattering channels satisfy the restrictions $k_z > k_c$ and $k_z' < -k_c$.

VI. Alkali Spectra

Figures 5-9 show the heterocontact spectral functions for all combinations of the five alkali metals Li, Na, K, Rb, and Cs. For the purpose of comparison with the material 1 portion of each heterocontact function, figures 5, 7, 8, and 9 show one-half of the homocontact spectrum for Li, Na, K, and Rb, respectively. (One half of the homocontact spectrum is the portion caused by scattering in material 1.) In many of the spectra (Rb Cs being a notable exception), the phonon structure of the two materials is well separated in energy, a great advantage in analyzing the spectra. All five figures illustrate the two main effects caused by increasing k_c : the decrease in magnitude of the material 1 portion of the spectra, and the decrease in relative magnitude of the highest energy peak. We comment on the reasons for each of these effects in turn.

The cause of the decrease in overall magnitude of the spectra for contacts to a material with smaller bandwith, particularly dramatic in the case of Na and K (Figures 6 and 7), is simply the reduced scattering implied by the restrictions $k_z > k_c$ and $k_z' < -k_c$. First, of course, scattering with $\Theta_{k,k'} < \Theta_{\min}$ is eliminated from $G(\omega)$ which decreases the magnitude of $G(\omega)$. Second, the number of channels with $\Theta_{k,k'} > \Theta_{\min}$ is reduced as k_c grows, further decreasing the magnitude of $G(\omega)$.

The different behavior of the different metals is due to the different strengths of $2k_F$ scattering relative to small angle scattering. Quantitatively, the ratio

$|V(2k_F) - V(0)|$ measures the relative strength of $2k_f$ scattering; the value of this ratio is .273 for Li, .025 for Na, .057 for K, .172 for Rb, and .272 for Cs. Thus in Na and K, $2k_F$ scattering is weak and does not contribute a large part of the spectrum. As a result, the effect of eliminating scattering with $\Theta_{\vec{k},\vec{k}'} < \Theta_{\min}$ is a sharp decrease in the overall magnitude of the Na and K spectra.

The decrease in relative magnitude of the highest energy peak compared to other peaks in the spectra is particularly visible in the Li spectra (Fig. 5). This effect is related to the amount that $2k_F$ scattering contributes to each peak in the spectra: if the contribution of $2k_F$ scattering to the highest energy peak is smaller than to the other peaks, the exclusion of scattering with $\Theta_{\vec{k},\vec{k}'} < \Theta_{\min}$ will affect the highest energy peak more than the others. To show the relative importance of $2k_F$ phonons to the different spectral peaks, we have plotted in Figure 10 the effective density of states of $2k_F$ phonons, $f_{eff}(\omega)$, in Li. By the effective density of states, we mean the density of states obtained by weighting each $2k_F$ state by the factor $(2\vec{k}_F \cdot \vec{e}_{2\vec{k}_F,\lambda})^2/\omega_{2\vec{k}_F,\lambda}$ which appears in the electron phonon matrix element (Eq.(19)). Notice that the contribution of $2k_F$ scattering to the highest energy peak is smaller than to any other peak. As $2k_F$ scattering becomes more dominant for increasing $\Theta_{\min}$, the point contact spectral function should approach the shape of $f_{eff}(\omega)$. Figure 10 shows the Li/Li and Li/Cs spectral functions normalized like $f_{eff}(\omega)$ so each has a maximum value of 1.0; the Li/Cs spectrum ($\Theta_{\min}$=109.2°) is indeed more like $f_{eff}(\omega)$ in shape than the Li/Li spectrum ($\Theta_{\min}$=0).

VII. Concluding Remarks

We conclude that point contact spectroscopy in the heterocontact case measures a substantially different spectral function than in the homocontact case, corresponding to a different weighted average of the scattering rate over the Fermi surface. The weight factor we have calculated for free electron metals in the absence of interfacial scattering (Eq. (7) and (8)) restricts the observed scattering in material 1 to that between initial states with $k_z > k_c$ and final states with $k_z' < -k_c$, where $k_c = \sqrt{2m(\mu_1 - \mu_2)}\ \hat{n}$ is the transverse wavevector necessary to cross the internal potential barrier. The weight factor for scattering in material 2 is the same as in the homocontact. Application of the heterocontact weight factor to the calculation of realistic alkali metal spectra shows that the heterocontact weight factor has a dramatic effect on the spectra, an effect that should be experimentally observable. First, the relative strength of the material 1 portion of the spectra decreases relative to the material 2 portion as k_c increases. Second, the shape of the material 1 portion changes so that $2k_F$ phonon scattering is more prominent as k_c increases.

While we have derived results only for free electron metals, it is possible to extend the results in a speculative way to more realistic systems. The feature of the heterocontact problem that leads to a substantially different weight factor is the restrictions on which electrons can enter material 2 from 1 and on which states electrons enter when crossing from material 2 to 1. In free electron metals, these restrictions are neatly given in terms of k_c as in the last paragraph, or equivalently by the requirement that momentum parallel to the interface is conserved. Clearly at a real, possibly disordered interface the crystal momentum

parallel to the interface is not necessarily conserved. A simple model of interfacial scattering (δ-function barrier) indicates that scattering at the interface changes the shape of the signal and the relative contributions of scattering in material 1 and 2.[9] At a realistic interface, to the extent that parallel crystal momentum is conserved, there will be severe restrictions on electrons passing between two materials with very different Fermi surface sizes (ie., different k_F's). These restrictions will lead to a heterocontact weight factor that is substantially different from the homocontact one (though perhaps not given by Eqs.(6)-(8)) and may lead to observable differences in the point contact spectrum. We suggest that the Al/In heterocontact is a fruitful system for future experimental and theoretical work because the Fermi surfaces are relatively simple, the values of k_F are sufficiently different (10-15%), and the phonon spectra are reasonably well separated in energy ($\Theta_D = 394$ K for Al, 129 K for In).

Acknowledgments

The authors would like to thank John Wilkins for many useful discussions and Roger Taylor for providing some of the computer code used in the calculations. This work was supported in part by the U.S. Office of Naval Research.

References

1. A. G. M. Jansen, A. P. van Gelder, and P. Wyder, J. Phys. C **13** , 6073 (1980).

2. A. G. M. Jansen, J. H. van der Bosch, H. van Kempen, J. H. J. M. Ribot, P. H. H. Smeets, and P. Wyder, J. Phys. F **10** , 265 (1980).

3. Yu. G. Naidyuk, I. K. Yanson, A. A. Lysykh, and O. I. Shklyarevskii, Fiz. Twerd. Tela (Leningrad) **22** , 3665 (1980) (Sov. Phys. Solid State **22** , 2145 (1980)).

4. I. O. Kulik, A. N. Omel'yanchuk, R. I. Shekter, Fiz. Nizk. Temp. **3** ,1543 (1977) (Sov. J. Low Temp. Phys. **3** , 740 (1977)).

5. A. P. van Gelder, Solid State Com. **35** , 19 (1980).

6. A. G. M. Jansen, F. M. Mueller, and P. Wyder, Phys. Rev. B **16** , 1325 (1977).

7. A. G. Batrak and I. K. Yanson, Fiz. Nizk. Temp. **5** , 1401 (1979) (Sov. J. Low. Temp. Phys. **5** , 663 (1979)).

8. H. U. Baranger and J. W. Wilkins, in **The Physics of Submicron Structures** , edited by H. L. Grubin, K. Hess, G. J. Iafrate and D. K. Ferry (Plenum Publishing Corporation, 1984) p. 295.

9. R. I. Shekter and I. O. Kulik, Fiz. Nizk. Temp. **9** , 46 (1983) (Sov. J. Low Temp. Phys. **9** , 22 (1983)).

10. We have neglected the change in electric field, $E = E^{*} + \delta E$. A small change in the electric field will significantly affect only trajectories which go near the edge of the hole. There are not many of such trajectories and we

therefore neglect this effect; see Kulik, et al. reference 4.

11. Notice that once one assumes that $|\vec{v}(s)| = v_F$ and that the paths of the electrons are straight, $\vec{k}$ is no longer dependent on t' as indicated in Eq. (12) but rather is simply a dummy variable.

12. A. H. MacDonald, J. Phys. F **10** , 1737 (1980).

13. As an example of the uncertainty in quantitive results when one makes the free electron approximation in Li and Cs, in reference 12 the effect of the larger effective mass in Li and Cs on the value of λ $(=2\int d\omega G(\omega)/\omega)$ was estimated to be about 30% in Li and 20% in Cs.

14. A. H. MacDonald and C. R. Leavens, Phys. Rev. B **26** , 4293 (1982).

15. R. C. Shukla and R. Taylor, J. Phys. F **6** , 531 (1976).

16. L. Dagens, M. Rasolt, and R. Taylor, Phys. Rev. B **11** , 2726 (1975).

17. R. Taylor, Can. J. Phys. **60** , 725 (1982).

TABLE I. The minimum scattering angle in material 1, Θ_{min}, for pairs of alkali metals. Θ_{min} is defined by $\sin(\Theta_{min}/2)=k_c/k_{F1}=\sqrt{2m(\mu_1-\mu_2)}/\hbar k_{F1}$. The Fermi wavevector, k_{F2}, is listed below each material; a dash in the table signifies $\mu_1<\mu_2$.

material 1		material 2				
		Li	Na	K	Rb	Cs
	k_{F2} (Å^{-1})	1.121	.923	.745	.693	.645
Li		0	67.8°	95.8°	101.8°	109.2°
Na		-	0	72.0°	81.8°	91.3°
K		-	-	0	41.7°	60.3°
Rb		-	-	-	0	44.5°

Figure Captions

Fig. 1. Ideal interface between two metals. (a) The conduction bands in equilibrium are shown. $\Delta=\mu_1-\mu_2$ is the intrinsic barrier seen by electrons coming from the left. (b) The equilibrium distribution just to the left and just to the right of the interface are shown. $k_c=\sqrt{2m(\mu_1-\mu_2)}/\hbar$ is the critical wavevector: electrons must have $k_z>k_c$ to pass from material 1 to material 2, and electrons in material 1 which came from material 2 must have $k_z<-k_c$. Electrons in the shaded regions will cross the interface; those in the hatched regions have crossed the interface; those in the blank region stay in metal 1.

Fig. 2. Point contact of radius a under a forward bias without scattering. The distribution function $f^{n\sigma}(\vec{r},\vec{k})$ for electrons is shown at 6 points in space. The x indicates the point in space at which the distribution in $\vec{k}$ is drawn. Shaded and hatched regions are as in figure 1. The shape of $f^{n\sigma}$ severely restricts the possible electron-phonon scattering events: the initial state in material 1 must have $k_z>k_c$ in order for the scattering event to affect the current, and any empty final state must have $k_z'<-k_c$. The indicated angle Θ_{min}, defined by $\sin(\Theta_{min}/2)=k_c/k_{F1}$, is the smallest angle of scattering in metal 1 that contributes to decreasing the current.

Fig. 3. The regions of space for calculating ΔI due to the electron-phonon interaction. $T(\vec{k}_1)$ (vertical shading) is the half-tube parallel to $\vec{k}_1$ upstream from the hole, while $T(\vec{k}_2)$ (plus shading) is the corresponding tube for $\vec{k}_2$. $\overline{T}(\vec{k}_1)$ (X shading) and $\overline{T}(\vec{k}_2)$ (horizontal shading) are the downstream complements of $T(\vec{k}_1)$ and $T(\vec{k}_2)$ respectively. The contribution of scattering between $\vec{k}_1$ and $\vec{k}_2$ to $\Delta I^{(1)}$, the change in current in material 1, comes from the intersection of $T(\vec{k}_1)$ and $\overline{T}(\vec{k}_2)$ (grid shading). Likewise, the contribution to $\Delta I^{(2)}$, the change in current in material 2, comes from the intersection of $T(\vec{k}_2)$ and $\overline{T}(\vec{k}_1)$ (starred shading).

Fig. 4. The ratio of the weight factor for scattering in material 1, $W^{(1)}(q)$, to that for scattering in material 2, $W^{(2)}(q)$ as a function of the magnitude of the phonon wavevector $q = 2k_F \sin(\Theta_{\vec{k},\vec{k}'}/2)$. $W^{(2)}(q)$ is equal to one-half of the homocontact weight factor ($\frac{1}{4}(1-\Theta_{\vec{k},\vec{k}'}/\tan\Theta_{\vec{k},\vec{k}'})$, where $\Theta_{\vec{k},\vec{k}'} = \cos^{-1}(\hat{k}\cdot\hat{k}')$). Curves are shown for four values of the the critical value of the wavevector, $k_c = \sqrt{2m(\mu_1-\mu_2)}/\hbar$: $k_c/k_{F1} =$ 0.1, 0.5, 0.7, and 0.9. $W^{(1)}(q)$ is zero for q less than $2k_c$, so that scattering through angles less than Θ_{min} does not contribute to the spectral function. $W^{(1)}(q)$ is smaller than $W^{(2)}(q)$ for all q because the restrictions $k_z > k_c$ and $k_z' < -k_c$ reduce the amount of scattering at every q. As in the homocontact case, $W^{(1)}(q)$ diverges at $q = 2k_{F1}$, enhancing the effect of $2k_{F1}$ phonons.

Fig. 5. The spectral function, $G(\omega)$, for a Li Na contact (dotted line) and a Li Cs contact (solid line) compared to one-half of the Li homocontact spectral function (dashed line). The magnitude of the Li portion of the spectrum decreases as the bandwith of the second material, μ_2, decreases because the phase space for scattering becomes more restricted. The shape of the Li portion changes as μ_2 decreases reflecting the increasing importance of $2k_F$ phonons and the lack of small angle scattering. In particular, the relative height of the high energy peak decreases. The shape of the Na and Cs portions of the spectrum is the same as in the homocontact case; however, the normalization differs by the ratio v_{F2}/v_{F1}.

Fig. 6. The spectral function, $G(\omega)$, for Li K contact (dashed line), a Li Rb contact (solid line), and a Li Cs contact (dotted line, the same as in Fig. 5). In the case of the Li Rb and Li Cs contacts, the Li portion of the spectra is well separated from the Rb and Cs portion. The spectrum of the Li K contact has a particularly large peak near 9 meV because the highest energy K peak and lowest energy Li peak nearly coincide. The spectra for energies above 10 meV clearly show the effect of the changing weight factor.

Fig. 7. The spectral function, $G(\omega)$, for a Na/Cs contact (solid line), a Na/Rb contact (dotted line), and a Na/K contact (dashed-dotted line) compared to one-half of the Na homocontact spectral function (dashed line). Because the form factor for $2k_F$ scattering is particularly small in Na, the effect of the smaller bandwidth materials on the Na portion of the spectra is dramatic: the magnitude of the Na portion decreases sharply and the height of the highest energy Na peak is reduced relative to the rest of the Na spectrum.

Fig. 8. The spectral function, $G(\omega)$, for a K/Cs contact (solid line) and a K/Rb contact (dotted line) compared to one-half of the spectrum for a K homocontact (dashed line). As in the case of Na shown in Fig. 7, the weakness of scattering by $2k_F$ phonons in K leads to a sharp decrease in the K portion of the spectra as μ_2 decreases.

Fig. 9. The spectral function, $G(\omega)$, for a Rb/Cs contact (solid line) compared to one-half of the spectrum from a Rb homocontact (dashed line). The Rb and Cs portions of the spectrum overlap considerably leading to a complicated structure. However, as in the other conbinations of alkalis, the change in weight factor causes a decrease in the highest energy Rb peak.

Fig. 10. The effective $2k_F$ density of states, $f_{eff}(\omega)$, for Li (solid line) compared to one-half of the Li homocontact spectrum (dashed line) and to the Li Cs spectrum (dotted line), all normalized so that their maximum value is 1. $f_{eff}(\omega)$ is the fraction of $2k_F$ phonons with frequencies between ω and $\omega + d\omega$ weighted by $(2\vec{k}_F \cdot \vec{v}^{\,2}_{2\vec{k}_F,\lambda} / \omega_{2\vec{k}_F,\lambda})$. The shape Li Cs spectrum, in which $2k_F$ phonons are emphsized because small angle scattering is eliminated, is much more like that of $f_{eff}(\omega)$ than is the Li homocontact spectrum.

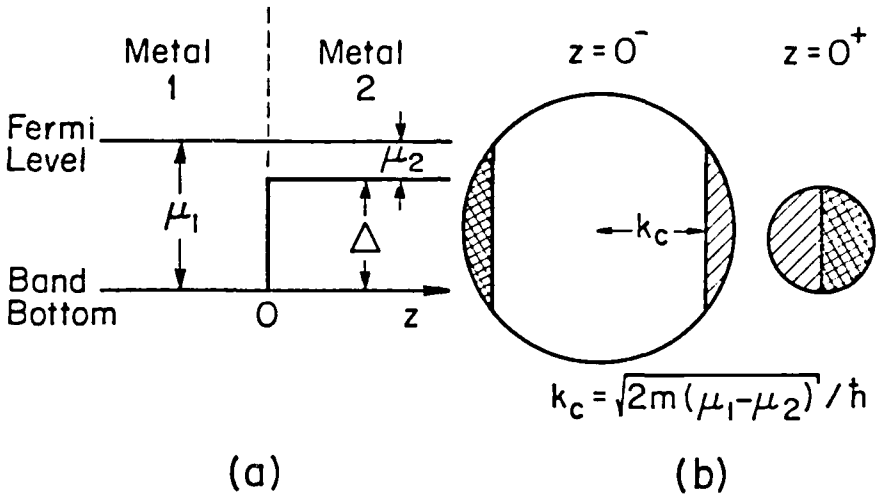
Metal 1
Metal 2
Fermi Level
μ_2
μ_1
Δ
Band Bottom
0
z
$z = 0^-$
$z = 0^+$
k_c
$k_c = \sqrt{2m(\mu_1 - \mu_2)}/\hbar$
(a)
(b)

Fig. 1

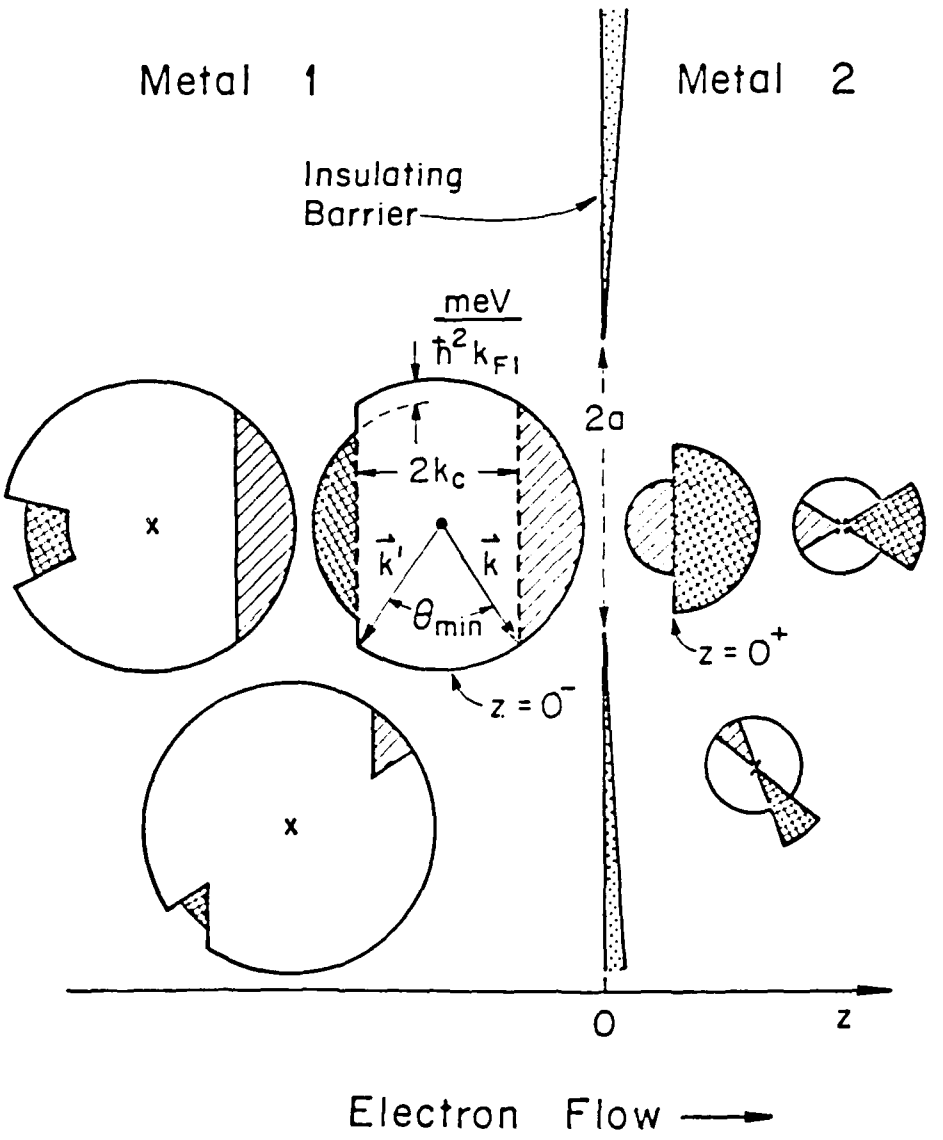
Metal 1
Metal 2
Insulating Barrier
meV
$\hbar^2 k_{F1}$
2a
$2k_c$
$\vec{k}'$
$\vec{k}$
θ_{min}
x
x
$z = 0^-$
$z = 0^+$
0
z
Electron Flow

Fig. 2

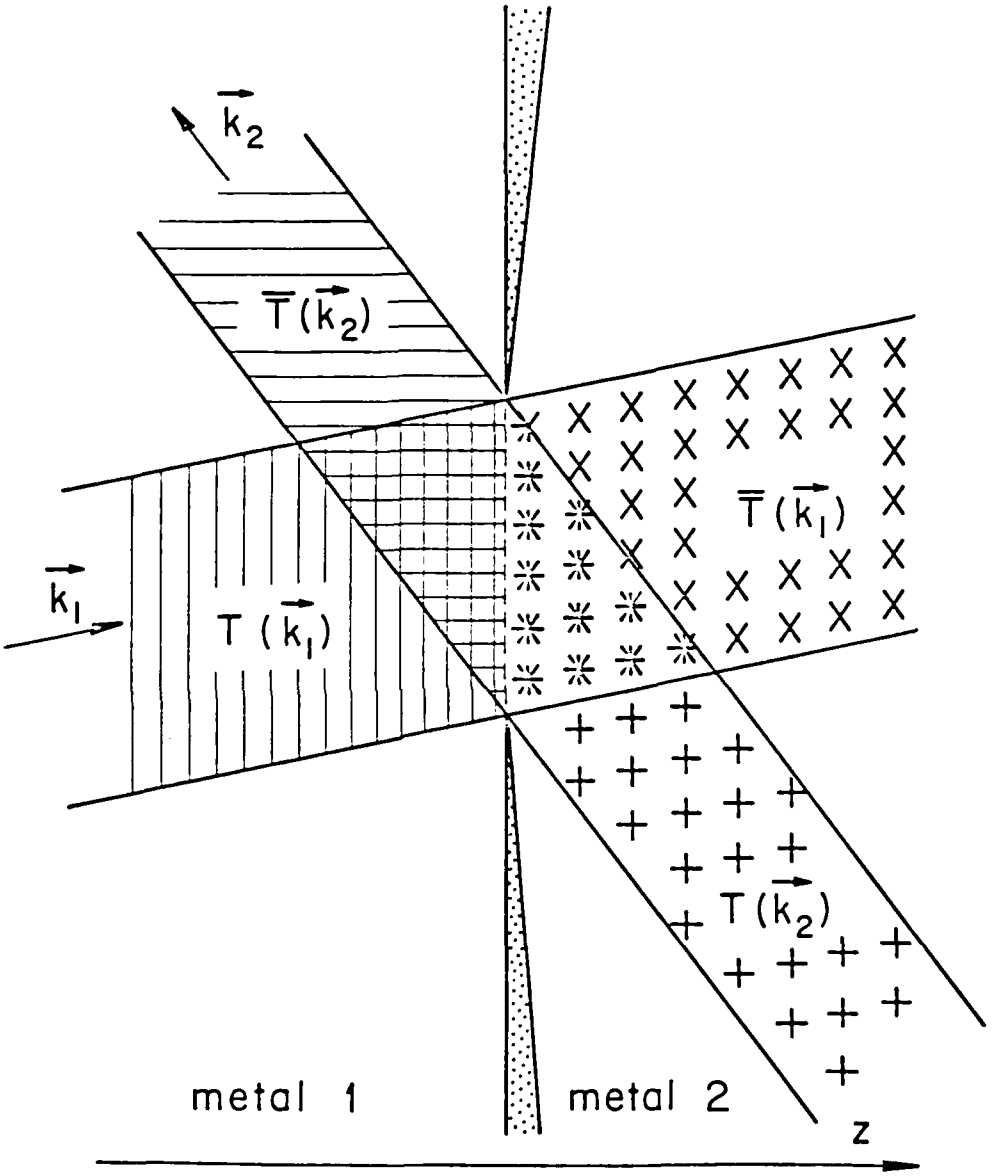
$\vec{k}_2$
$\bar{T}(\vec{k}_2)$
$\bar{T}(\vec{k}_1)$
$\vec{k}_1$
$T(\vec{k}_1)$
$T(\vec{k}_2)$
metal 1
metal 2
z

Fig. 3

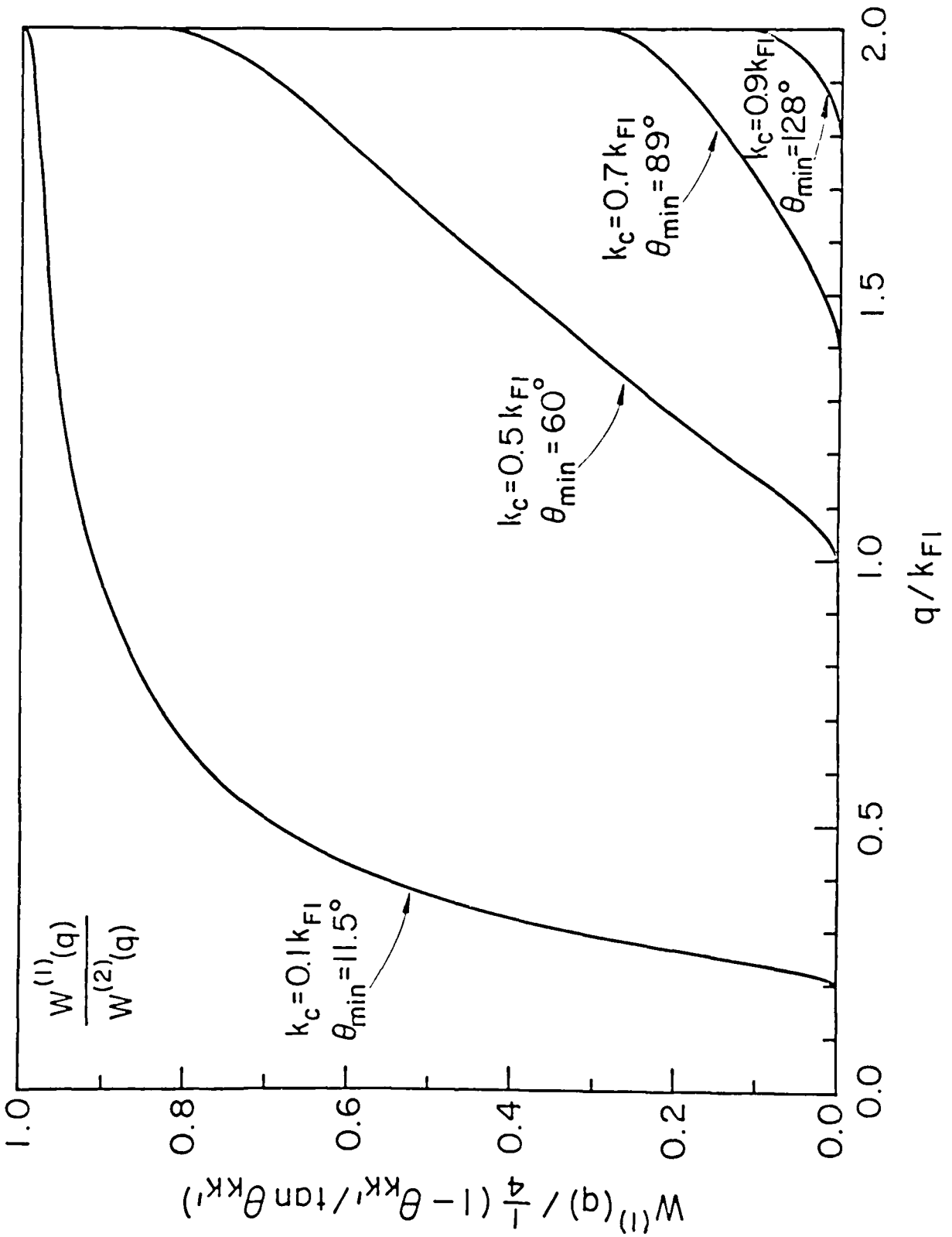
$W^{(1)}(q) / \frac{1}{a^1} (1 - \theta_{kk'} / \tan\theta_{kk'})$
1.0
0.8
0.6
0.4
0.2
0.0
0.0
0.5
1.0
1.5
2.0
q / k_{FI}
$\frac{W^{(1)}(q)}{W^{(2)}(q)}$
$k_c = 0.1\, k_{FI}$
$\theta_{min} = 11.5°$
$k_c = 0.5\, k_{FI}$
$\theta_{min} = 60°$
$k_c = 0.7\, k_{FI}$
$\theta_{min} = 89°$
$k_c = 0.9 k_{FI}$
$\theta_{min} = 128°$

Fig. 4

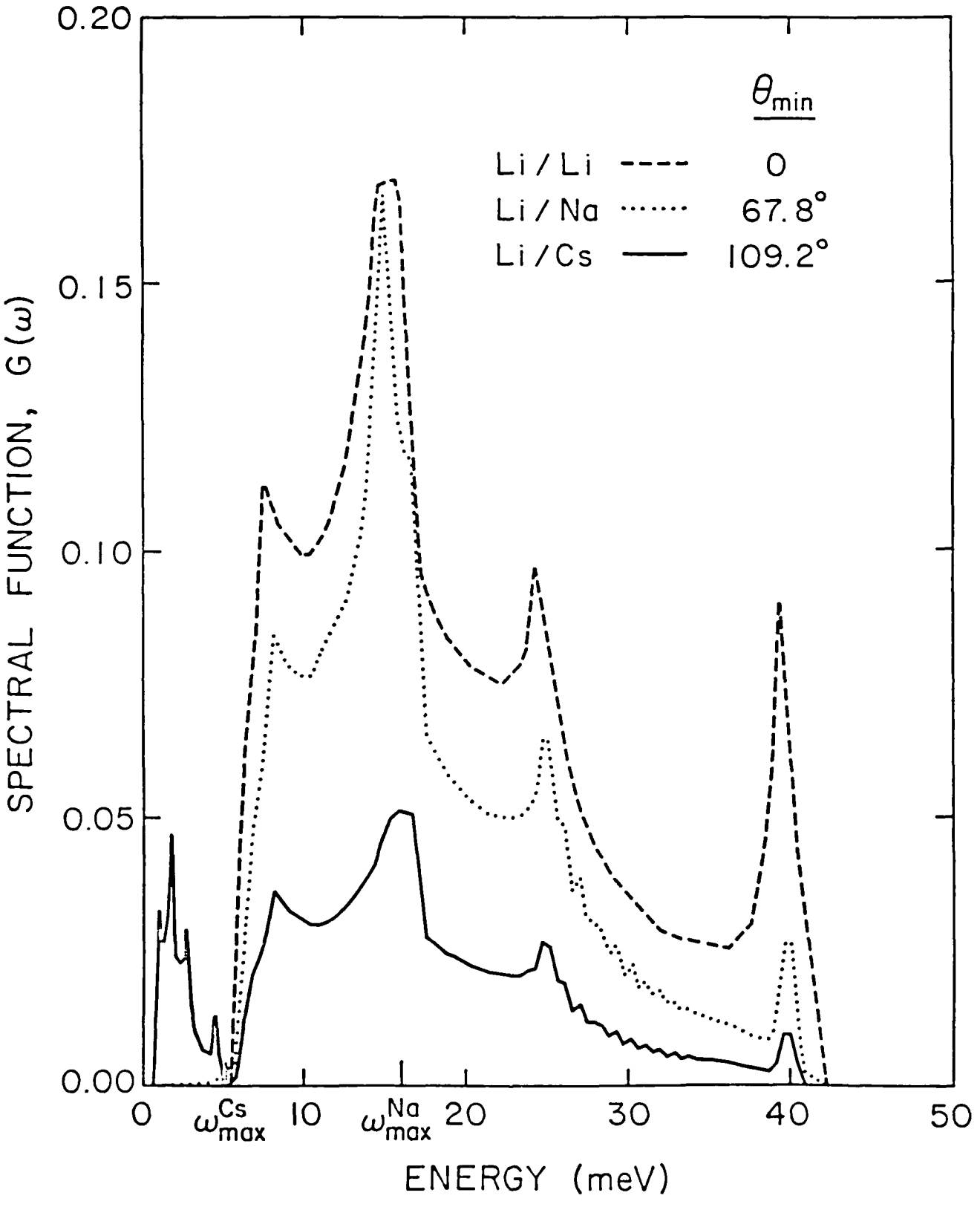
0.20
0.15
0.10
0.05
0.00
SPECTRAL FUNCTION, G(ω)
θmin
Li/Li ---- 0
Li/Na ····· 67.8°
Li/Cs —— 109.2°
0
ωCs max
10
ωNa max
20
30
40
50
ENERGY (meV)

Fig. 5

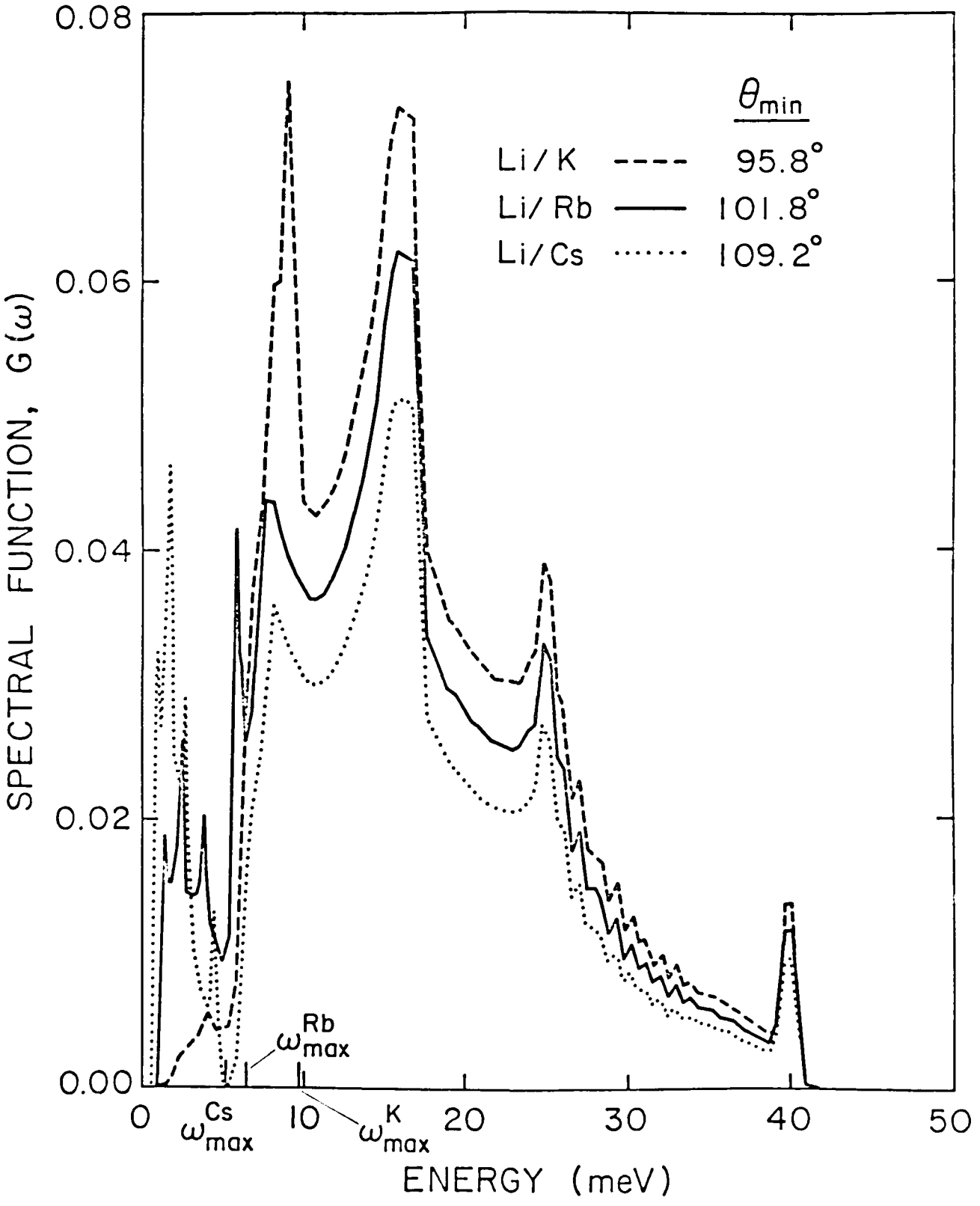
0.08
0.06
0.04
0.02
0.00
SPECTRAL FUNCTION, G(ω)
θmin
Li/K ---- 95.8°
Li/Rb —— 101.8°
Li/Cs ····· 109.2°
ωRb max
ωCs max
ωK max
0
10
20
30
40
50
ENERGY (meV)

Fig. 6

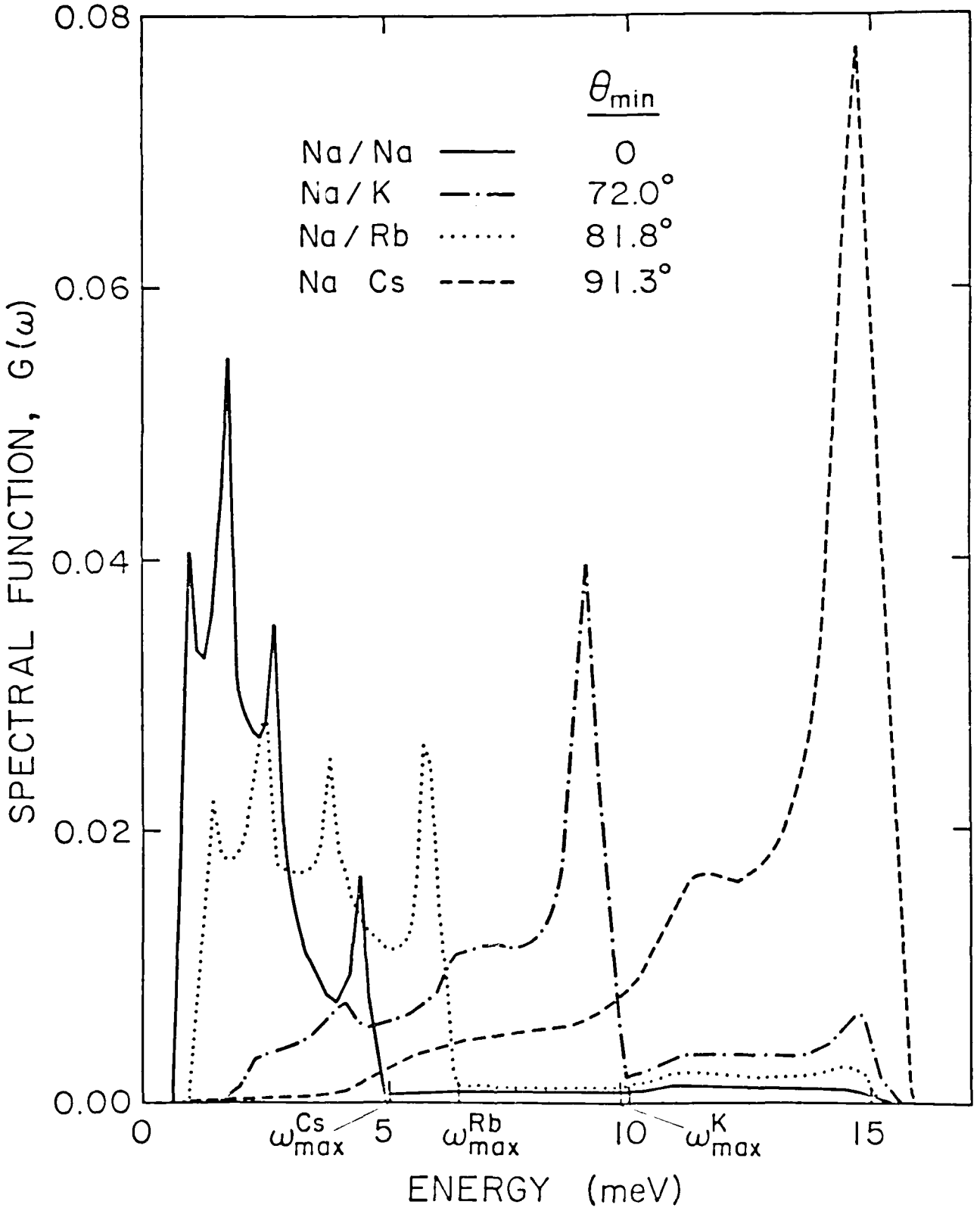
0.08
0.06
0.04
0.02
0.00
SPECTRAL FUNCTION, G(ω)
θmin
Na/Na 0
Na/K 72.0°
Na/Rb 81.8°
Na Cs 91.3°
0
5
10
15
ω^Cs_max
ω^Rb_max
ω^K_max
ENERGY (meV)

Fig. 7

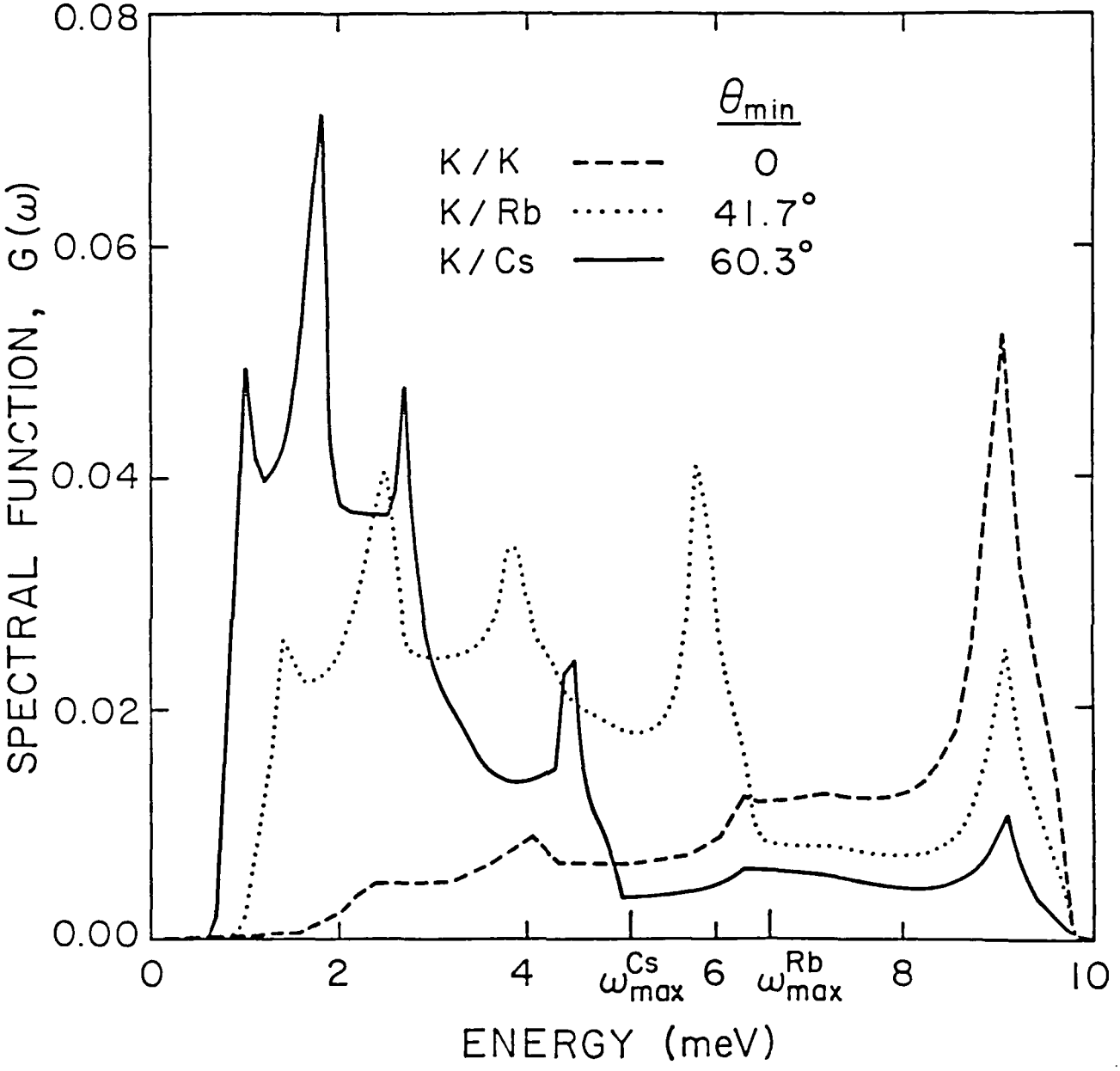
0.08
0.06
0.04
0.02
0.00
SPECTRAL FUNCTION, G(ω)
θmin
K/K ---- 0
K/Rb ····· 41.7°
K/Cs —— 60.3°
0
2
4
ωCs max
6
ωRb max
8
10
ENERGY (meV)

Fig. 8

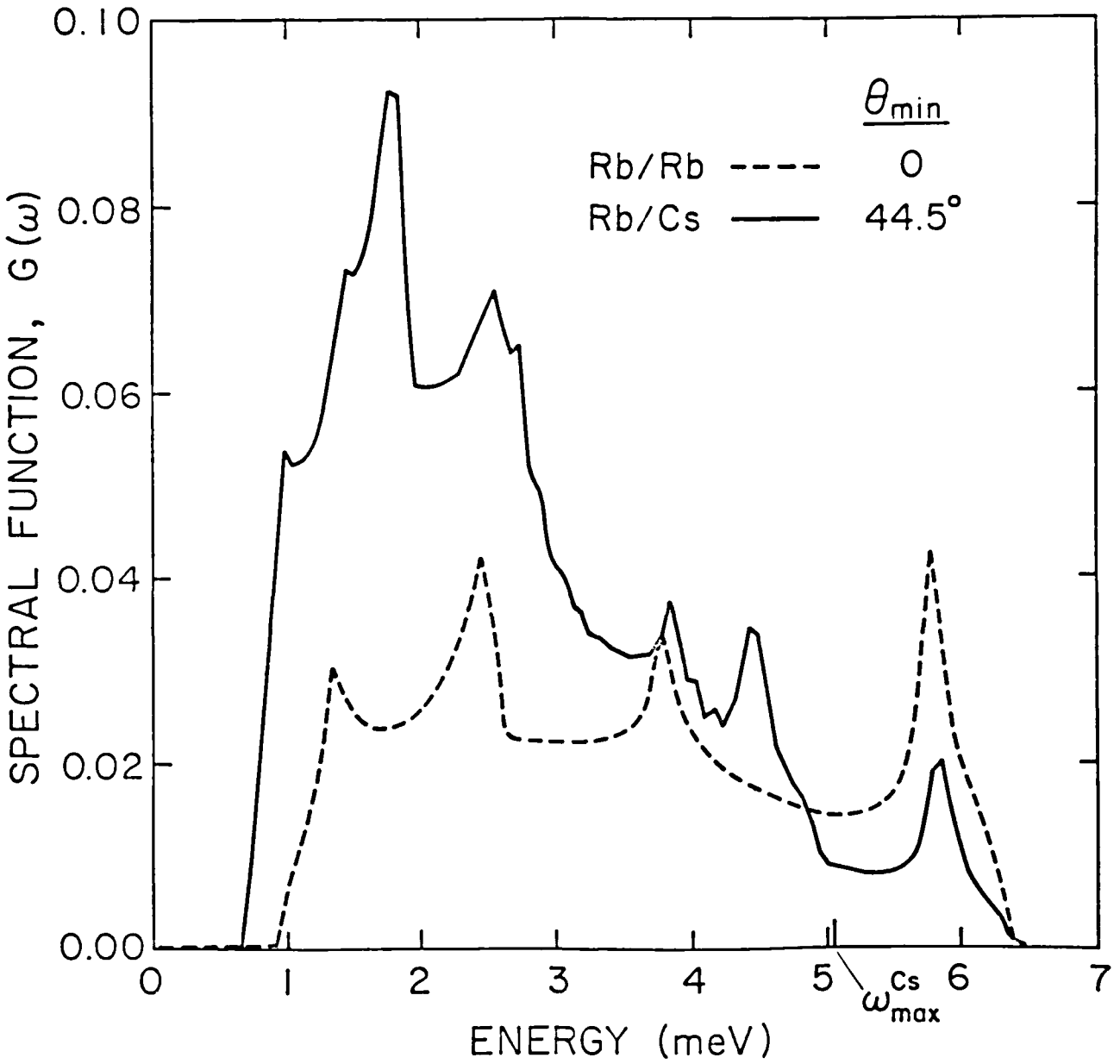
0.10
0.08
0.06
0.04
0.02
0.00
SPECTRAL FUNCTION, G(ω)
θmin
Rb/Rb ---- 0
Rb/Cs —— 44.5°
0
1
2
3
4
5
6
7
ωmax Cs
ENERGY (meV)

Fig. 9

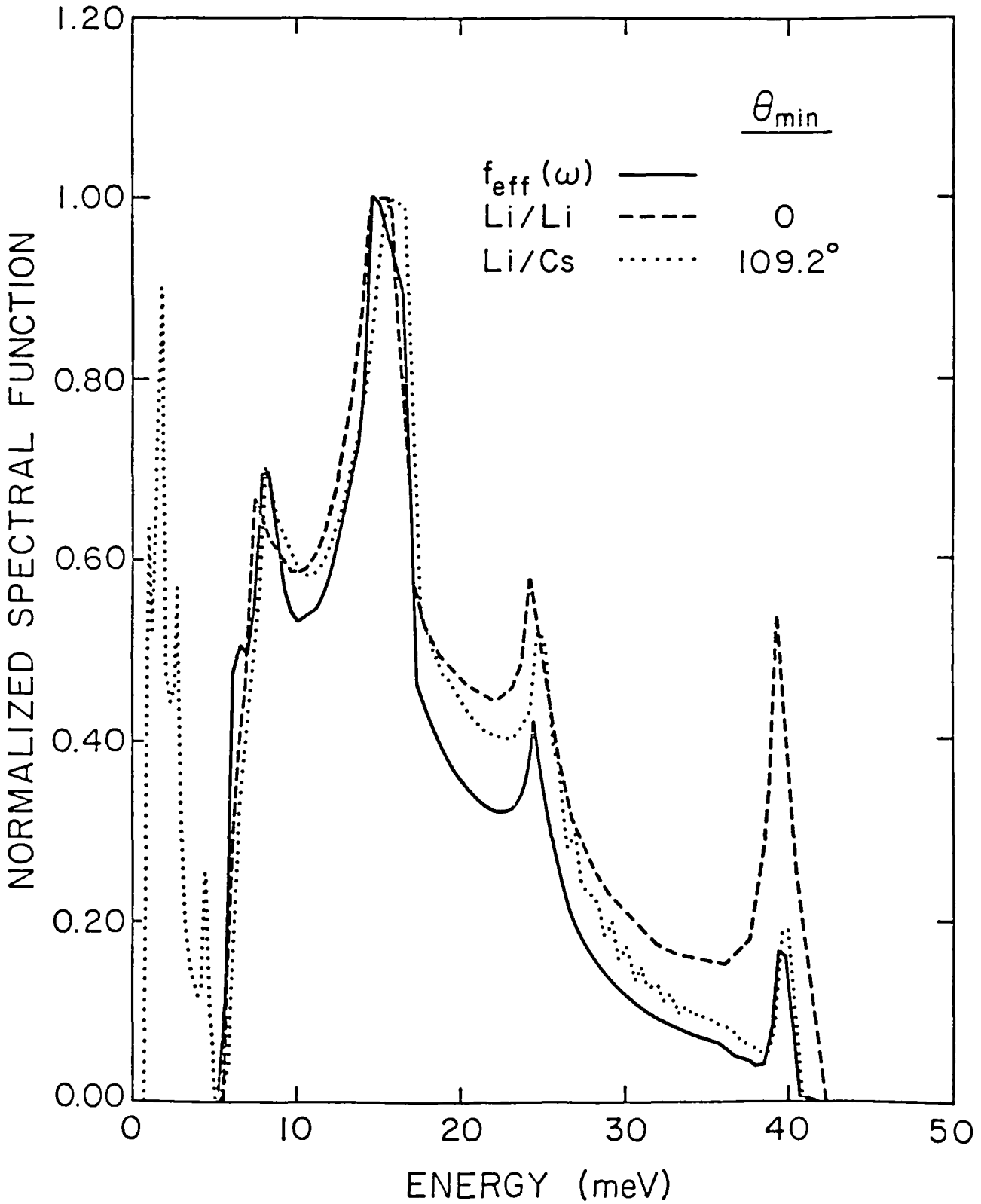
1.20
1.00
0.80
0.60
0.40
0.20
0.00
NORMALIZED SPECTRAL FUNCTION
0
10
20
30
40
50
ENERGY (meV)
θmin
feff (ω)
Li/Li
Li/Cs
0
109.2°

Fig. 10

END

FILMED

2-85

DTIC